Quantitative Proteome Analysis of Mouse Liver Lysosomes Provides Evidence for Mannose 6-phosphate-independent Targeting Mechanisms of Acid Hydrolases in Mucolipidosis II*⃝S

Sandra Markmann‡§§, Svenja Krambeck‡§§, Christopher J. Hughes§, Mina Mirzaian¶, Johannes M.F.G. Aerts¶, ⦿ Paul Saftig‖, Michaela Schweizer, Johannes P.C. Vissers§, Thomas Braulke‡ ‡‡, and ⦿ Markus Damme‖‡‡**

The efficient receptor-mediated targeting of soluble lysosomal proteins to lysosomes requires the modification with mannose 6-phosphate (M6P) residues. Although the absence of M6P results in misrouting and hypersecretion of lysosomal enzymes in many cells, normal levels of lysosomal enzymes have been reported in liver of patients lacking the M6P-generating phosphotransferase (PT). The identity of lysosomal proteins depending on M6P has not yet been comprehensively analyzed. In this study we purified lysosomes from liver of PT-defective mice and 67 known soluble lysosomal proteins were identified that illustrated quantitative changes using an ion mobility-assisted data-independent label-free LC-MS approach. After validation of various differentially expressed lysosomal components by Western blotting and enzyme activity assays, the data revealed a small number of lysosomal proteins depending on M6P, including neuraminidase 1, cathepsin F, Npc2, and cathepsin L, whereas the majority reach lysosomes by alternative pathways. These data were compared with findings on cultured hepatocytes and liver sinusoid endothelial cells isolated from the liver of wild-type and PT-defective mice. Our findings show that the relative expression, targeting efficiency and lysosomal localization of lysosomal proteins tested in cultured hepatic cells resemble their proportion in isolated liver lysosomes. Hypersecretion of newly synthesized non-phosphorylated lysosomal proteins suggest that secretion-recapture mechanisms contribute to maintain major lysosomal functions in liver. *Molecular & Cellular Proteomics 16: 10.1074/mcp.M116.063636, 438–450, 2017.*

Soluble lysosomal proteins undergo a specific modification on high-mannose type N-linked oligosaccharides for an efficient transport from the Golgi apparatus to late endosomes and lysosomes by phosphorylation of distinct mannose residues in the C6 position. This modification is catalyzed by the subsequent action of two enzymes: the first enzyme is an N-acetylglucosamine (GlcNAc)[1]-1-phosphotransferase (PT), which mediates the transfer of GlcNAc-1-phosphate from uridine diphosphate (UDP)-GlcNAc to mannose acceptors forming GlcNAc-phosphomannose diester (1–3). The second so called 'uncovering enzyme' removes GlcNAc to expose mannose 6-phosphate (M6P) residues (4). Two M6P-specific receptors (MPRs), MPR46 and MPR300, can bind M6P-modified lysosomal proteins in the *trans* Golgi network (TGN) and mediate their segregation from the secretory pathway (5). Lysosomal enzymes which escape the binding to MPRs are secreted but can be reinternalized by MPR300 localized at the plasma membrane and delivered to lysosomes via the endocytic pathway. MPR-ligand complexes reach late endosomal compartments where the acidic pH induces the dissociation of lysosomal cargo. MPRs are then transported back to the TGN or the plasma membrane for further rounds of transport (6).

PT is a heterohexameric enzyme complex consisting of two α-, two β-, and two γ subunits (7). The α- and β-subunits are encoded by the *GNPTAB* gene (8, 9), and the γ-subunits are coded by *GNPTG* (10). The α- and β-subunits contain the catalytic center for PT activity and the recognition sites for

[1] The abbreviations used are: GlcNAc, *N*-acetylglucosamine; ki, knock-in; M6P, Mannose 6-phosphate; MPRs, M6P receptors; ML II, mucolipidosis type II; PT, phosphotransferase; TGN, trans Golgi network; RAP, receptor-associated protein; LSECs, Sinusoid endothelial cells; UDP, uridine diphosphate; wt, wild-type.

lysosomal protein substrates and UDP-GlcNAc (11) whereas the role of the γ-subunits are less defined, but might be involved in the folding and stabilization of the PT complex, prerequisite for optimum catalytic activity, and selective recognition of subsets of lysosomal proteins (12, 13). Mutations in *GNPTAB* and *GNPTG* lead to lysosomal storage diseases, mucolipidosis type II (ML II also called I-cell disease) and III (ML III) (14). The failure or partial formation of M6P residues on soluble lysosomal proteins in ML II and ML III, respectively, impair their proper delivery to lysosomes and result in their hypersecretion into the extracellular space and bloodstream. The defect in mannose phosphorylation, however, allows processing of high mannose-type oligosaccharides to negatively charged complex-type units and the formation of abnormal proteolytically processed intracellular and secreted forms of lysosomal enzymes (15–17). Although all cells and tissues in ML II are deficient in PT activity, fibroblast and mesenchymal cells are most strikingly affected (18), indicating that these cells particularly rely on M6P-dependent lysosomal protein delivery pathways. In contrast, many cell types (such as hepatocytes, Kupffer cells and leukocytes) and several organs (liver, spleen, kidney and brain) have nearly normal level of lysosomal enzymes (18–21). These observations suggest the existence of lysosomal transport pathways that do not require M6P recognition marker on lysosomal enzymes.

We have generated previously a *Gnptab* knock-in (PT^{ki}) mouse model for ML II by insertion a mutation found in ML II patients which led to a complete loss of PT activity (17). These PT^{ki} mice show all biochemical and clinical symptoms of the human disease (17, 22, 23). Here we present a comprehensive quantitative proteomic approach of purified lysosomes ("tritosomes") from liver of wild-type (wt) and PT^{ki} mice. This allowed us to identify proteins for which M6P is indispensable for their proper delivery to lysosomes. We found proteins which are significantly decreased, as well as sets of proteins of similar or even increased expression in lysosomes from PT^{ki} mice in comparison with wild-type controls. The analytic data were biochemically evaluated and compared with primary cultured hepatocytes and sinusoid endothelial cells (LSECs). Further, pulse-chase experiments with cultured hepatic cells indicated that hypersecretion of nonphosphorylated lysosomal enzymes followed by M6P-independent recapture mechanisms are important for maintenance of lysosomal functions in ML II liver.

EXPERIMENTAL PROCEDURES

Antibodies and Materials—The Npc2 antiserum was a kind gift from Dr. Shutish Patel and described previously (24), Neu1 and Ppca antibodies were a kind gift from Dr. Allessandra D'Azzo (St. Jude Children's Research Hospital; Memphis), Mpr300 antibodies were a kind gift from Dr. Kurt von Figura (University of Göttingen) and β-glucuronidase antibody was kindly provided by Dr. William S. Sly (St. Louis University). Recombinant human arylsulfatase B (ARSB) was kindly provided by Dr. Michel Vellard (Biomarin/Genzyme, San Rafael, CA). The monoclonal Lamp1 (clone 1D4B) and Lamp2 (clone Abl93)

antibodies were purchased from the Developmental Studies Hybridoma Bank. Ctsd antiserum used for immunofluorescence analysis and immunoprecipitation was described previously (25). Antibodies against Ctsd for Western blotting, Ctsh, Ctsa, and Ctss were obtained from Santa Cruz (Dallas, TX). Ctsb was purchased from Neuromics, Ctsz, and Ctsl from R&D Systems (Minneapolis, MN), Lrp1 and Ldlr from Abcam. Chemicals were, if not stated otherwise, purchased from Sigma Aldrich (Cambridge, United Kingdom).

Mice—The PT^{ki} mouse model was generated by the insertion of a cytosine in position 3082 of the murine *Gnptab* gene (c.3082insC) (17). Mice were housed in a pathogen-free animal facility at the University Medical Center Hamburg-Eppendorf, and experimental procedures were performed according to the institutional guidelines and approved by the Amt für Gesundheit und Verbraucherschutz and the Ministerium für Landwirtschaft, Umwelt und ländliche Räume des Landes Schleswig-Holstein.

Isolation of Primary Hepatocytes and Liver Sinusoidal Endothelial Cells (LSECs)—Primary mouse hepatocytes were isolated by liver perfusion, EDTA dissociation and centrifugation on a Percoll gradient as described previously (26). LSECs were isolated as described previously (27).

Isolation of Lysosomes from Liver (Tritosomes)—Mice were injected with 4 μl/g bodyweight of a 17% (w/v in 0.9% NaCl) Triton WR1339 solution (Sigma Aldrich) 4 days prior to sacrifice. The livers were removed and homogenized in five volumes of ice-cold 0.25 M sucrose with three strokes with a Potter-Elvejhem homogenizer. The homogenates were centrifuged at 1000 × g for 10 min at 4 °C. After removal of the supernatant and resuspension of the pellet followed by another centrifugation step at 1000 × g for 10 min at 4 °C, the supernatants were pooled (post nuclear supernatant, PNS) and centrifuged in an ultracentrifuge at 56,000 × g (70.1 Ti rotor, Beckmann, Coulter, Indianapolis, IN) for 7 min at 4 °C. After rehomogenization of the pellet with 0.25 M sucrose followed by another ultracentrifugation step, the supernatant was discarded and the pellet was resuspended in sucrose solution with a density of 1.21 (resulting in the ML-fraction, representing the mitochondrial-lysosomal fraction). The ML fraction (~3.5 ml) was overlaid each with 2.5 ml sucrose solutions of 1.15, 1.14, and finally 1.06 density yielding a discontinuous sucrose gradient. After centrifugation at 110,000 × g for 150 min in a swinging bucket rotor (SW41 Ti rotor, Beckmann Coulter), lysosomes/tritosomes were collected at the interphase between ρ 1.14 and 1.06 sucrose (F2-fraction).

Western Blotting—Five micrograms (tritosome protein), 100 μg (total liver protein), or 25 μg hepatocytes or LSECs protein were separated by SDS-PAGE and blotted on nitrocellulose membranes. After blocking with low-fat milk powder for 30 min at room temperature, membranes were incubated with the primary antibodies over night at 4 °C. After further incubation with Horseradish peroxidase-coupled secondary antibodies, blots were developed with enhanced chemiluminescence solution. Densitometric analyses were performed with the ImageJ software (NIH) to quantify band intensities.

Two-dimensional Gel Electrophoresis—Two-dimensional gel electrophoresis was carried out essentially as described previously (28) with Immobiline DryStrip gels (IPG strip) (GE Healthcare Life Sciences) in a pH range of 4–7 and 400 μg of total tritosome protein.

Metabolic Labeling and Immunoprecipitation of Cathepsin D and Z—Cells grown on 35 mm dishes were metabolically labeled with 150 μCi/ml [^{35}S] methionine (Hartmann Analytik; 37 Bq/mmol)in methionine-free DMEM for 45 min. After removal of the radioactive medium, cells were either harvested or washed with PBS and chased for 5 h in DMEM containing 5% dialyzed fetal bovine serum (FBS). Cell extracts and media were analyzed by immunoprecipitation of cathepsin D and cathepsin Z followed by SDS-PAGE and fluorography (29).

Endocytosis of Arylsulfatase B (ARSB)—Human ARSB was iodinated with sodium [^{125}I] (Hartmann Analytik, Braunschweig, Germany, 74 TBq/mmol) and IODO-GEN® (Pierce, Waltham, MA) as described (30) to a specific activity of 22 μCi/μg. Hepatocytes grown in 35 mm dishes were preincubated with DMEM containing 0.1% bovine serum albumin (BSA) (DMEM/BSA) for 30 min, followed by incubation with [^{125}I]-labeled ARSB ($\sim$600,000 cpm/ml in DMEM/BSA) in the absence or presence of 10 mM M6P or 10 μM receptor associated protein (RAP) for 20 min at 37 °C as indicated. After washing, the cells were either harvested in 10 mM Tris/HCl, pH 7.4 containing 0.25 M sucrose or chased for 6 h in DMEM/BSA. The cells were solubilized in PBS containing 0.2% Triton X-100 and protease inhibitors, separated by SDS-PAGE and visualized by autoradiography.

Immunofluorescence Staining of Hepatocytes—Double immunofluorescence staining of hepatocytes was performed as described previously (31). For filipin staining the cells were stained with 1 μg/μl filipin in PBS.

Immunofluorescence Staining of Liver Sections—Formalin-fixed liver was equilibrated in 30% (w/v) sucrose in 0.1 M phosphate buffer (PB), pH 7.4 overnight and sectioned using a sliding microtome (SM2000R, Leica) into 30 μm thick free floating sections and collected in PB. After blocking in PB containing 0.5% Triton X-100 and 4% normal goat serum for 2 h at room temperature, sections were incubated with the primary antibodies in the blocking solution overnight at 4 °C. After washing three times in PB containing 0.25% Triton X-100 (washing solution), sections were incubated with fluorophore-coupled secondary antibodies (AlexaFluor 488 and 594; Molecular Probes, Waltham, MA) for one hour at room temperature. After additional three washing steps in washing solution, sections were coverslipped in Mowiol/DABCO. Confocal microscopy was performed on an Olympus FV1000 fluorescence microscope.

Enzyme Activity Measurements—Enzyme activity measurements were performed with liver homogenates, tritosomes, hepatocytes, and 24 h conditioned media. The liver was homogenized in 5 volumes of 50 mM Tris/HCl buffer pH 7.4 containing 0.25 M sucrose, 1 mM EDTA and protease inhibitors (Sigma) and centrifuged at 500 $\times$ *g* to remove all cell debris. After addition of 0.5% Triton X-100 the lysates were incubated for 1 h at 4 °C. Cultured hepatocytes were extracted directly in PBS containing 1% Triton X-100 and protease inhibitors. Activities of β-glucuronidase, α-L-iduronidase and α-L-fucosidase were measured in 0.1 M sodium citrate buffer pH 4.5 containing 0.15 M NaCl with 1 mM 4-methylumbelliferyl β-D-glucuronide (Sigma-Aldrich), 50 μM 4-methylumbelliferyl α-L-iduronide (Glycosynth) and 1 mM 4-methylumbelliferyl-α-L-fucopyranoside (Sigma-Aldrich), respectively. As enzyme source extracts of 50–100 μg liver tissue (50–100 μg protein), hepatocytes (25–70 μg protein), and tritosomes (5 μg protein) were added to the assay mixture to a final volume of 100 μl. After incubation for 2 to 24 h at 37 °C the reaction was stopped by addition of 900 μl 0.4 M glycine/NaOH buffer, pH 10.4.

Measurement of iduronate-2-sulfatase activity was performed as described previously (32). Using 100 and 5 μg protein of liver extracts and tritosomes, respectively, as enzyme source. The liberated 4-methylumbelliferone was measured fluorometrically (excitation at 355 nm and emission 460 nm) related to 4-MU standard solutions.

Protein Digestion—Each sample (20 μg of protein) was dissolved in 0.1% (w/v) RapiGest (Waters Corporation, Milford, MA) in 50 mM ammonium bicarbonate (Sigma Aldrich, St. Louis, MO) and heated at 80 °C for 45 min. The samples were reduced in the presence of 5 mM dithiotreitol (Sigma Aldrich) at 60 °C for 30 min and alkylated in the presence of 10 mM iodoacetamide (Sigma Aldrich) at ambient temperature in the dark for another 30 min. Proteolytic digestion was initiated by adding sequencing grade TMPK-treated trypsin (Promega, Madison, MI) at a 1:50 (w/w) ratio and incubation conducted for 4 h at 37 °C. A second aliquot of trypsin was added at a 1:50 (w/w)

ratio and followed by incubation overnight at 37 °C. TFA was added to a final concentration of 0.5% (v/v) in order to hydrolyze RapiGest and the solutions incubated at 37 °C for 20 min before being vortexed and centrifuged for 30 min at 13,000 rpm.

LC-MS Configuration—LC separations were performed with an ACQUITY M Class system (Waters Corporation), equipped with a Symmetry C18 5 μm, 2 cm $\times$ 180 μm precolumn and an HSS T3 C18 1.7 μm, 25 cm $\times$ 75 μm analytical column. The samples were transferred with aqueous 0.1% (v/v) formic acid to the precolumn at a flow rate of 5 μl/min. Mobile phase A was water containing 0.1% (v/v) formic acid, whereas mobile phase B was acetonitrile containing 0.1% (v/v) formic acid. The peptides were eluted from the precolumn to the analytical column and separated with a gradient of 3–40% mobile phase B over 90 min at a flow rate of 300 nl/min. The analytical column temperature was maintained at 35 °C. The lock mass compound, [Glu1]-Fibrinopeptide B (200 fmol/μl), was delivered at 600 nl/min to the reference sprayer of the mass spectrometer.

Mass spectrometric analysis of tryptic peptides was performed using a Synapt G2-Si mass spectrometer (Waters Corporation, Wilmslow, United Kingdom). The mass spectrometer was operated in v-mode with nominal resolution of 20,000 FWHM. All analyses were performed in positive mode ESI. The ion source block temperature and capillary voltage were set to 100 °C and 3.2 kV, respectively. The time of flight analyzer (ToF) of the mass spectrometer was externally calibrated with a NaCsI mixture from m/z 50 to 1990. LC-MS data were collected in mobility assisted data independent (UDMSE) mode of acquisition (33). The spectral acquisition time in each mode was 0.5 s with a 0.02 s interscan delay. In low energy mode, data were collected at constant Trap collision energy of 4 eV (per unit charge) and a constant Transfer collision energy of 2 eV (per unit charge). In elevated energy mode, the Trap collision energy was ramped from 4 eV to 5 eV (per unit charge) in 0.5 s, and the Transfer collision energy was set to ramp during each 14 ms ion mobility separation, with the ramp applying the optimum collision energy for species at a particular drift time. The ion mobility separations were combined in a 0.5 s total elevated energy integration time. The reference sprayer sampled every 60 s and the data post-acquisition lock mass corrected.

Data Processing and Database Searching—ProteinLynx Global-SERVER v3.0.2 (Waters Corporation) was used to process the acquired data. Protein identifications were obtained by searching a Mus Musculus UniProt database (16,674 reviewed entries, release 2014_10). To assess protein and peptide FDR values, decoy database entries were created by reversing the amino acid sequences and concatenating them with the original database entries. The principle of the search algorithm has been described (34). Peptide and fragment ion tolerances were determined automatically, equaling 5 and 10 ppm respectively, one missed cleavage allowed, as well as fixed carbamidomethylation modification of cysteine and variable oxidation modification of methionine. ISOQuant was applied for the integrated quantitative analysis of data derived from multiple LC-MS runs (http://www.isoquant.net). The results have been deposited to the Proteome Xchange Consortium (http://proteomecentral.proteomexchange.org) via the PRIDE partner repository (35) with the data set identifier PXD001556.

Experimental Design and Statistical Rationale, Statistics, Hierarchical Clustering, Enrichment Analysis, and Principal Component Analysis—The experimental design comprised four biological and three technical replicates of PT^{ki} and WT each, a number adequate enough to detect small changes in the protein abundance in the tritosome samples with sufficient statistical power. Two-tailed unpaired Student's *t*-tests were calculated using Excel (tables) or Graphpad Prism (graphs). The protein abundance data from WT and PT^{ki} mice followed a normal distribution. Errors bars represent the means $\pm$ S.E. of mean (S.E.). For annotation of proteomics data as heat maps,
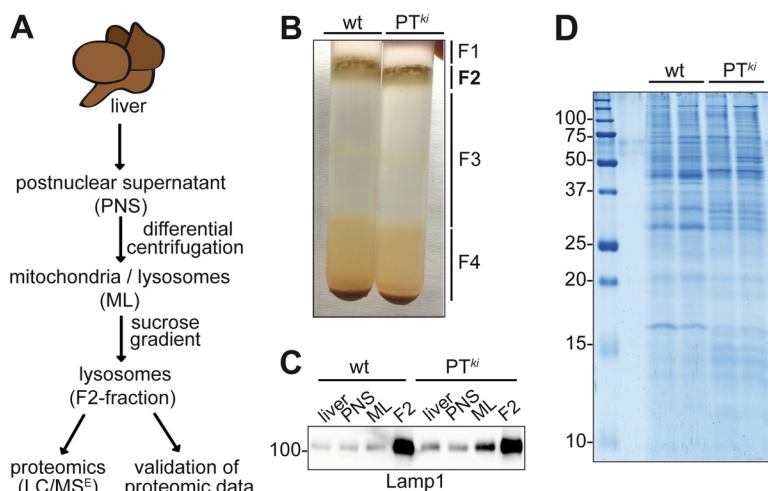
FIG. 1. **Subcellular fractionation and purification of lysosomal fractions for proteomic analysis.** *A*, Schematic diagram of the applied workflow for subcellular fractionation of lysosomes from mouse liver. *B*, Representative photographs of the discontinuous sucrose gradients of mitochondria and lysosome-enriched fractions (*ML*) from wt and PT^{ki} mice. The positions of F1 to F4 fractions of the gradient are indicated. The F2-fraction (*bold*) is the lysosome-enriched fraction used for further experiments. *C*, Western blotting analysis of liver extracts and the different subcellular fractions (25 μg protein) from wt and PT^{ki} mouse liver reveal the enrichment of the lysosomal marker protein Lamp1. *PNS*, postnuclear supernatant; *ML*, mitochondria/lysosomes; *F2*, lysosome-enriched fraction. *D*, Coomassie Blue stained SDS gel (15% acrylamide) used to separate each 20 μg of lysosomal F2 fraction from two wt and PT^{ki} animals. The positions of molecular mass marker proteins in kDa are indicated.

GENE-E software was used (http://www.broadinstitute.org/cancer/software/GENE-E). Both columns and rows were hierarchically clustered and the "one minus Pearson correlation" was chosen as the column distance metric. Principal component analysis was performed by ClustVis (36). For functional annotation of the proteomics data, the "Database for Annotation, Visualization and Integrated Discovery" (DAVID) was used and the "Functional Annotation Chart" was chosen for enrichment-analysis of KEGG pathways (37).

RESULTS

Proteomic Analysis of Isolated Liver Lysosomes—Early studies measuring the activities of few lysosomal hydrolases in liver tissue of ML II patients have revealed nearly normal levels (19, 20). In order to determine the impact of the loss of M6P targeting signals on the lysosomal proteome in the liver, Triton WR1339-filled lysosomes (tritosomes) were purified from the liver of wt and PT^{ki} mice by differential and subsequent discontinuous sucrose gradient centrifugation (Fig. 1*A*; (38)). Western blotting analysis of liver lysates and different fractions obtained showed highest enrichment of lysosomes in the F2-fraction characterized by the lysosomal membrane protein Lamp1. The enrichment and yield of tritosomes were comparable between wt and PT^{ki} preparations (Fig. 1*B* and 1*C*). One-dimensional SDS-PAGE and Coomassie Blue staining of wt and PT^{ki} lysosomes, however, revealed significant differences in intensity and band pattern (Fig. 1*D*). Separation of the lysosomal F2 fractions by 2D gel electrophoresis followed by Coomassie staining indicated additional differences in the composition of the lysosomal proteome between wt and PT^{ki} mouse liver, such as the amounts and isoform pattern for lysosomal proteases tripeptidyl peptidase 1 (Tpp1), cathepsin H (Ctsh), Ctsz, Ctsb, and Ctsd (supplemental Fig.

S1). The altered charges and molecular masses of proteins in PT^{ki} lysosomes are most likely because of differences in complex type oligosaccharides and proteolytic modifications (15, 39). Because 2D gel electrophoresis resolve only the most abundant lysosomal proteins representing a small part of the proteome (28), quantitative label-free LC-/MS (ion mobility-assisted data independent analysis (UDMSE (33)) was applied to tritosome samples purified from four different animals of each genotype from distinct littermates. The protein amounts were estimated by expressing summed peptide intensity responses *versus* that of an exogenous protein spike (40), and normalized, to account for experimental differences, to the total tritosome protein content and expressed as μg/g tritosome protein values. About 900 proteins have been identified in the lysosomal F2 fractions of wt and PT^{ki} animals, but among them lysosomal proteins represent half of the most abundant 150 proteins (supplemental Table S1). The numerous nonlysosomal proteins identified here represent mostly mitochondrial, cytosolic as well as intermediate filament proteins that we considered as contaminants (supplemental Fig. S2). However, we cannot exclude that several of these proteins may reach lysosomes via the degradative autophagy pathway. Hierarchical clustering of the list of selected soluble lysosomal proteins revealed clear differences in the levels of most proteins between wt and PT^{ki} mice (Fig. 2*A*). Principal component analysis (PCA) of the soluble lysosomal proteins showed a clear separation of the two genotypes (Fig. 2*B*). Furthermore, sigmoidal plot of all identified proteins demonstrated differential protein levels for a number of proteins including soluble lysosomal enzymes like Neu1 and Ctsf
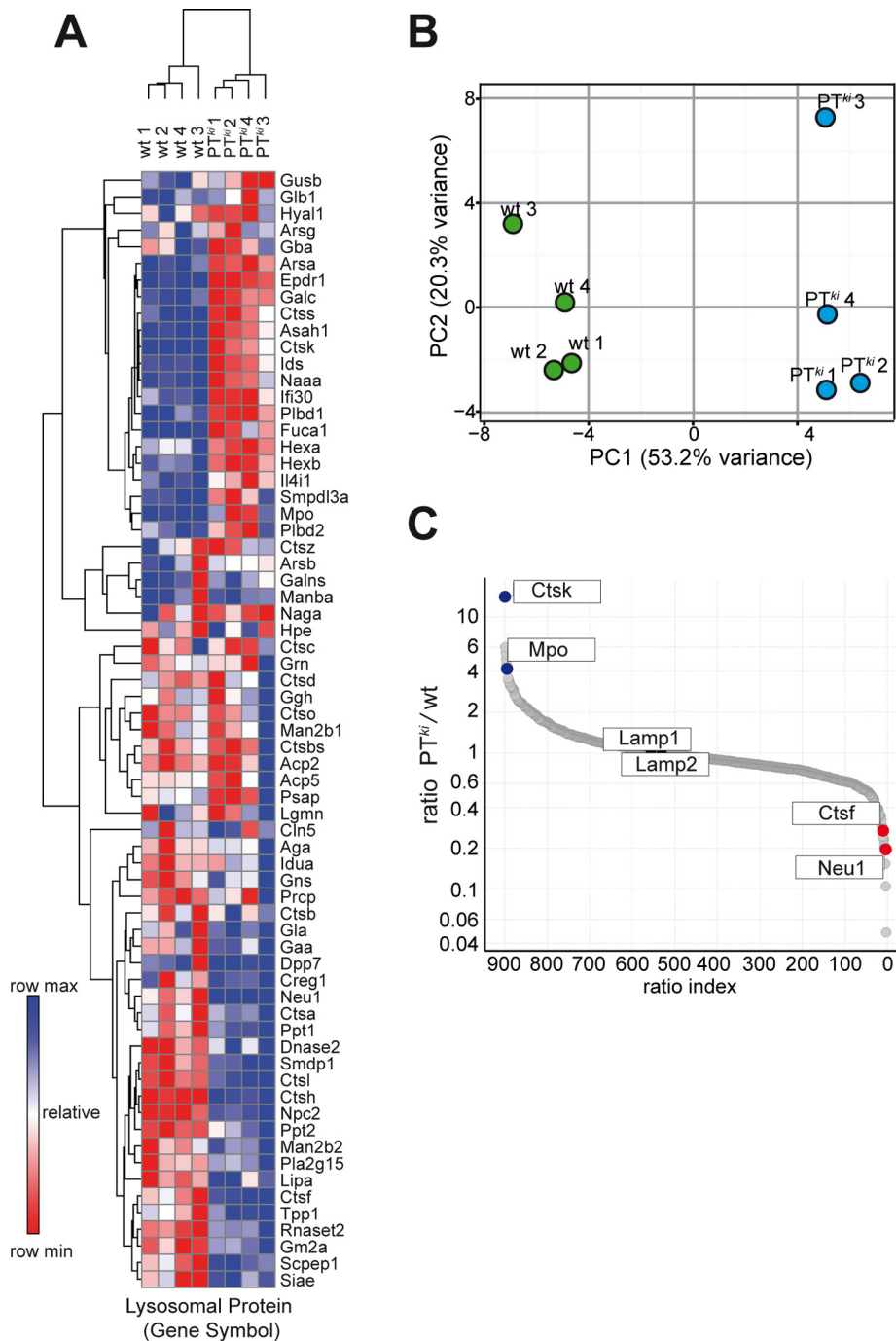
FIG. 2. **Global proteomic change analysis of lysosome-enriched fractions from wt and PT^{ki} mouse liver.** *A*, Heat map representation and hierarchical clustering of 67 soluble lysosomal proteins identified and quantified by LC/MS^E in at least five out of eight animals. Clustering of color-coded lysosomal proteins of the individual animals of each genotype is shown. *Blue*, higher protein amount than wt; *red*, lower protein amount than wt. *B*, Principal component analysis (PCA) of the proteome data analyzed for soluble lysosomal proteins shows clear separation of the two genotypes (wt1–4, *green spots*, PT^{ki}1–4, *blue spots*) and the close grouping of the individual animals. Percentage variance for each principal component is given. *C*, Sigmoidal plot of all 902 identified proteins shows differential protein levels for a number of proteins. The spots representing Ctsk, Mpo, Lamp1, Lamp2, Neu1 and Ctsf are highlighted.

which are decreased in PT^{ki} mice. Others such as the lysosomal membrane proteins Lamp1 and Lamp2 proteins were unchanged, whereas a number of soluble proteins like Ctsk and Mpo were found to be increased in PT^{ki} mice (Fig. 2C).

Among the identified proteins, 67 soluble lysosomal proteins described previously were found (41, 42) with the exception of sulfamidase (Gns), α-N-acetylglucosaminidase (Naglu) and arylsulfatase K (Arsk), whose expression was too

low (Table I). The quantitative analysis revealed a high dynamic range of more than two orders of magnitude in the average amounts of the different lysosomal protein species in wt mice. The most abundant proteins were granulin (Grn; 23 pg/ng tritosome protein), recently assigned to be localized in lysosomes (43), prosaposin (Psap; 19 μg/g tritosome protein), followed by cathepsin D (Ctsd; 18 μg/g), α-glucosidase (Gaa; 14 μg/g), and α-mannosidase (Man2b1; 13 μg/g). The lowest amounts of lysosomal proteins were measured for cathepsin K (Ctsk), iduronate-2 sulfatase (Ids) and arylsulfatase G (Arsg), ranging between 130 and 200 ng/g tritosome protein.

The levels of only five soluble lysosomal proteins in PT^{ki} tritosomes were found to be lower than 50% in PT^{ki} in comparison with wt tritosomes. This subset includes neuraminidase 1 (Neu1), cathepsin F (Ctsf), Niemann Pick type C 2 protein (Npc2), cathepsin L1 (Ctsl), and sphingomyelin phosphodiesterase 1 (Smpd1). A number of additional proteins showed significant, but less pronounced decrease in PT^{ki} lysosomes. The majority of lysosomal proteins showed no or only marginal differences in their concentration in tritosomes between wt and PT^{ki} mice. Surprisingly, the level of 13 lysosomal proteins was increased in tritosomes of PT^{ki} mice. This was most striking for cathepsin K (Ctsk) (1400%, $p = 4.35 \times 10^{-4}$). In addition to these established lysosomal proteins, we identified a number of soluble proteins, for which a lysosomal residency was suggested (42, 44). These include e.g. biotinidase, plasma α-L-fucosidase, serum amyloid P-component, or ribonuclease UK114 (supplemental Table S2). However, the levels of none of them were significantly affected in PT^{ki} mice.

Abundant lysosomal membrane proteins like Lamp1, Lamp2, Limp2, and Npc1 showed no differences in their total levels in tritosomes between wt and PT^{ki} mice (Table I, supplemental Table S3). A total of 45 known and 33 putative lysosomal membrane proteins (supplemental Table S3 and S4), identified previously in tritosomes (45), were detected and quantified. Additional 64 proteins known to function in endosomal and lysosomal trafficking processes were covered by our proteomic analysis (supplemental Table S5).

Expression Levels of Lysosomal Proteins—In order to validate our lysosomal proteomic dataset, we examined the expression of soluble lysosomal proteins and enzymes by Western blotting and enzyme activity assays. As shown in Fig. 3 the amount of immunoreactive polypeptides Neu1, Npc2, Ctsl, Ctsh, and Ctsa were significantly reduced in tritosomes of PT^{ki} mice. The expression of Ctsb, Ctsd, Ctsz, and β-glucuronidase (Gusb), as well as the lysosomal membrane protein Lamp1, were not or only marginally affected. Of note, for Ctsb and Ctsd changes in the proportion of single chain (sc), and their cleaved heavy (hc) and light chain (lc) forms were observed. The relative amounts of Ctss was elevated in PT^{ki} tritosomes in comparison to wt fractions (Fig. 3). The data for these selected lysosomal proteins were in complete agreement with the MS data analysis (Table I). For a number of lysosomal enzymes we additionally determined the specific

activity in extracts of both liver tissue and tritosomes. Both iduronate 2-sulfatase (Ids) and Fuca1 activities were 2- to 3-fold higher in liver tissue as well as tritosomes of Pt^{ki} mice than of wt animals (Fig. 4A) corresponding to the increased protein level of these enzymes. No significant changes where observed for Gusb and Idua (Fig. 4A). No or only modest changes in the mRNA levels of Npc2, Idua, Fuca1, Ctsk, Neu1, Ctsf, and Ids were observed in liver tissue (supplemental Fig. S3A) whereas the respective lysosomal proteins were increased or decreased, respectively, in tritosomes of PT^{ki} mice (Table I). These data excluded transcriptional regulation rather than posttranslational sorting events to explain the different concentrations of these lysosomal proteins in lysosomal fractions, which might be representative for the other lysosomal components. Western blotting analyses of whole liver lysates generally resembled the protein expression level in purified lysosomes, indicating that the bulk of these proteins are found in lysosomes (supplemental Fig. S3B).

Distribution of Lysosomal Proteases in Liver Tissue—To evaluate whether the almost unchanged concentrations of the lysosomal proteases Ctsd, Ctsb, and Ctsz in liver tissue or tritosomes between wt and PT^{ki} mice are caused by differential distribution in parenchymal cells (hepatocytes) and non-parenchymal cells (Kupffer cells, stellate cells, liver sinusoid endothelial cells (LSECs)), we performed immunofluorescence staining on liver sections. Ctsd, Ctsz, and Ctsb were found to be colocalized with the lysosomal marker protein Lamp1 both in wt and PT^{ki} hepatocytes representing the major cell type in liver tissue (Fig. 4B). Ctsl, however, that was reduced in PT^{ki} tritosomes to 40% of wt fractions, was almost absent in PT^{ki} hepatocytes but expressed in nonparenchymal cells (Fig. 4B).

Cultured Hepatic Cells—To examine differences in the composition of lysosomes between wt and PT^{ki} on the cellular level in more detail, we analyzed the steady state concentration, transport and sorting efficiency, and lysosomal localization of selected soluble lysosomal proteins in cultured hepatocytes and LSECs. Western blotting analysis revealed the almost complete loss of mature Npc2 from PT^{ki} hepatocytes, and the concomitant accumulation of Npc2 precursor polypeptides in the medium (Fig. 5A). Surprisingly, no accumulation of filipin-positive nonesterified cholesterol was observed in PT^{ki} hepatocytes (supplemental Fig. S4A) suggesting that the residual amounts of Npc2 are sufficient to mediate the egress of lipoprotein-derived cholesterol from lysosomes. Similarly, to the tritosome data, the steady state concentration of Neu1 was strongly reduced in PT^{ki} hepatocytes, whereas comparable amounts of Ctsb and Ctsz were found in hepatocytes of both genotypes. Different proteolytically processed forms of Ctsl and Ctsd were observed in wt and PT^{ki} hepatocytes. The latter lack the 20 kDa mature Ctsl form and exhibit a distinct proteolytic processing of single chain and heavy chain Ctsd forms. For both Ctsl (short exposure)

TABLE I

List of soluble and selected lysosomal membrane proteins identified in wt and PT_{ki} liver lysosomes

Proteins known to be components of lysosomes (41, 44) are given. The total levels for each protein in $\mu g/g$ tritosome protein is the average of $n = 4$. The fold change is given as the ratio between the mean PT^{ki}/wt. ns = not significant, $p < 0.05 = *$; $p < 0.01 = **$; $p < 0.001 = ***$.

| accession	gene name	description	max. score	reported peptides #	sequence coverage %	average wt [μg/g]	average PT^{ki} [μg/g]	ratio PT^{ki}/wt	t-test [p-value]	significance level
O35657	Neu1	Neuraminidase 1	5754	12	48	740	141	0.19	5.7E-04	***
Q9R013	Ctsf	Cathepsin F	6399	12	42	2114	544	0.26	1.9E-03	**
Q9Z0J0	Npc2	Niemann Pick C protein 2	29948	8	51	632	213	0.34	9.2E-06	***
P06797	Ctsl	Cathepsin L1	11987	11	57	1843	705	0.38	1.9E-05	***
Q04519	Smdp1	Sphingomyelin phosphodiesterase	4390	23	55	2112	952	0.45	1.4E-04	***
P49935	Ctsh	Cathepsin H	31386	16	69	5040	2525	0.50	3.3E-07	***
Q60648	Gm2a	Ganglioside GM2 activator	23475	10	79	759	440	0.58	1.6E-03	**
Q9CQ01	Rnaset2	Ribonuclease T2	16446	12	50	631	379	0.60	6.3E-04	***
O35448	Ppt2	Lysosomal thioesterase PPT2	10810	11	54	1164	708	0.61	1.3E-03	**
O89023	Tpp1	Tripeptidyl-peptidase 1	13692	14	48	8897	5751	0.65	9.6E-03	*
P56542	Dnase2	Deoxyribonuclease-2-alpha	3833	13	49	622	405	0.65	2.6E-03	**
Q8VEB4	Pla2g15	Group XV phospholipase A2	8017	16	59	1611	1061	0.66	4.1E-03	**
Q9Z0M5	Lipa	Lysosomal acid lipase	12092	19	66	3843	2682	0.70	3.2E-03	**
P48441	Idua	Alpha-L-iduronidase	1216	15	36	794	563	0.71	3.2E-02	*
O88531	Ppt1	Palmitoyl-protein thioesterase 1	35876	17	61	3564	2606	0.73	4.3E-03	**
Q920A5	Scpep1	Retinoid-inducible serine carboxypeptidase	18717	20	48	6338	4677	0.74	3.5E-03	**
P70665	Siae	Sialate O-acetylesterase	7495	20	55	3531	2668	0.76	7.5E-03	**
O54782	Man2b2	Epididymis-specific alpha-mannosidase	7624	31	53	12977	9866	0.76	3.3E-03	**
Q8BM88	Ctso	Cathepsin O	2308	7	30	299	231	0.77	2.1E-01	ns
Q64191	Aga	N(4)-(beta-N-acetylglucosaminyl)-L-asparaginase	18595	12	63	2148	1676	0.78	2.9E-02	*
Q8BFR4	Gns	N-acetylglucosamine-6-sulfatase	10917	22	55	4406	3450	0.78	7.1E-03	**
P16675	Ctsa	Lysosomal protective protein / Cathepsin A	21919	23	79	10410	8271	0.79	1.6E-02	*
P51569	Gla	Alpha-galactosidase A	7734	19	57	1095	876	0.80	4.7E-02	*
Q9ET22	Dpp7	Dipeptidyl peptidase 2	11678	19	53	4254	3505	0.82	9.1E-02	ns
Q6YGZ1	Hpe	Heparanase	1719	16	40	687	589	0.86	2.1E-01	ns
P70699	Gaa	Lysosomal alpha-glucosidase	18281	41	73	23787	20390	0.86	8.1E-03	**
P10605	Ctsb	Cathepsin B	49242	15	59	6266	5412.6	0.86	1.2E-02	*
O88668	Creg1	Cellular Repressor Of E1A-Stimulated Genes 1	13199	9	68	1622	1410	0.87	1.5E-02	*
P24638	Acp2	Lysosomal acid phosphatase	6406	13	34	1526	1339.5	0.88	3.7E-01	ns
Q3UMW8	Cln5	Ceroid-lipofuscinosis neuronal protein 5	4698	19	53	459	402	0.88	2.9E-01	ns
Q7TMR0	Prcp	Lysosomal Pro-X carboxypeptidase	10969	18	39	2192	1955	0.89	3.6E-02	*
Q8K2I4	Manba	Beta-mannosidase	9695	46	65	8391	7529	0.90	3.9E-01	ns
P18242	Ctsd	Cathepsin D	62387	20	69	12410	11454	0.92	1.8E-01	ns
Q9Z0L8	Ggh	Gamma-glutamyl hydrolase	5221	13	42	469	436	0.93	6.8E-01	ns
O09159	Man2b1	Lysosomal alpha-mannosidase	13154	44	59	22597	21187	0.94	1.8E-01	ns
P28798	Grn	Granulins	31173	18	52	23464	22186	0.95	4.3E-01	ns
Q8R242	Ctbs	Di-N-acetylchitobiase	10679	15	45	1417	1345	0.95	6.6E-01	ns
Q571E4	Galns	N-acetylgalactosamine-6-sulfatase	6342	25	72	1189	1131	0.95	8.3E-01	ns
O89017	Lgmn	Legumain	22205	16	50	7983	7728	0.97	4.5E-01	ns
Q05117	Acp5	Tartrate-resistant acid phosphatase type 5	38100	12	56	3747	3656	0.98	7.4E-01	ns
P97821	Ctsc	Dipeptidyl peptidase 1	26510	13	41	7636	7522	0.99	8.1E-01	ns
Q9WUU7	Ctsz	Cathepsin Z	30560	11	51	3477	3471	1.00	9.8E-01	ns
Q61207	Psap	Prosaposin	13006	29	55	17895	18009	1.01	8.9E-01	ns
P50429	Arsb	Arylsulfatase B	10460	25	61	3254	3313	1.02	8.8E-01	ns
Q9QWR8	Naga	Alpha-N-acetylgalactosaminidase	17942	26	66	2044	2102	1.03	6.7E-01	ns
Q91ZJ9	Hyal1	Hyaluronidase-1	2233	7	20	1147	1224	1.07	4.8E-01	ns
Q3TCN2	Plbd2	Putative phospholipase B-like 2	12230	22	62	6337	6794	1.07	1.3E-01	ns
P29416	Hexa	Beta-hexosaminidase subunit alpha	15163	26	59	4726	5293	1.12	1.2E-02	*
P23780	Glb1	Beta-galactosidase	7447	26	54	4168	4738	1.14	1.5E-01	ns
P12265	Gusb	Beta-glucuronidase	16124	29	68	7287	8317	1.14	1.0E-01	ns
Q3TYD4	Arsg	Arylsulfatase G	609	8	24	173	205	1.18	3.0E-01	ns
P17439	Gba	Glucosylceramidase	15730	22	70	3170	3765	1.19	2.8E-01	ns
P50428	Arsa	Arylsulfatase A	8640	16	58	1829	2292	1.25	2.8E-04	***
Q9ESY9	Ifi30	Gamma-interferon-inducible lysosomal thiol reductase	10420	7	45	810	1018	1.26	2.2E-03	**
Q8VCI0	Plbd1	Phospholipase B-like 1	22302	28	52	5421	7032	1.30	5.8E-04	***
P70158	Smpdl3a	Acid sphingomyelinase-like phosphodiesterase 3a	16486	11	40	1939	2819	1.45	3.3E-02	*
P20060	Hexb	Beta-hexosaminidase subunit beta	14389	26	67	3839	5954	1.55	5.6E-04	***
O70370	Ctss	Cathepsin S	34716	14	62	2936	4909	1.67	1.3E-03	**
P54818	Galc	Galactocerebrosidase	9907	22	57	2651	5433	2.05	1.7E-04	***
O09046	Il4i1	L-amino-acid oxidase	1555	14	33	249	541	2.17	3.0E-03	**
Q99M71	Epdr1	Mammalian ependymin-related protein 1	16842	13	50	289	642	2.22	1.7E-06	***
Q9D7V9	Naaa	N-acylethanolamine-hydrolyzing acid amidase	3494	12	51	250	565	2.26	2.5E-03	**
Q99LJ1	Fuca1	Tissue alpha-L-fucosidase	1859	13	38	215	525	2.45	2.3E-03	**
Q9WV54	Asah1	Acid ceramidase	16195	23	62	821	2134	2.60	3.5E-04	***
Q08890	Ids	Iduronate 2-sulfatase	1022	7	20	129	362	2.80	6.4E-04	***
P11247	Mpo	Myeloperoxidase	3182	24	35	303	1225	4.04	2.8E-02	*
P55097	Ctsk	Cathepsin K	7411	13	42	74	1000	13.53	4.3E-04	***
Selected lysosomal membrane proteins										
P11438	Lamp1	Lysosome-associated membrane glycoprotein 1	16442	11	34	4632	4574.9	0.988	8.5E-01	ns
P17047	Lamp2	Lysosome-associated membrane glycoprotein 2	13533	13	48	7846	7589.9	0.967	6.0E-01	ns
O35114	Scarb2	Lysosome membrane protein 2	18965	19	61	8627	8298.4	0.962	5.9E-01	ns
O35604	Npc1	Niemann-Pick C1 protein	5689	34	38	29428	28470	0.967	7.7E-01	ns
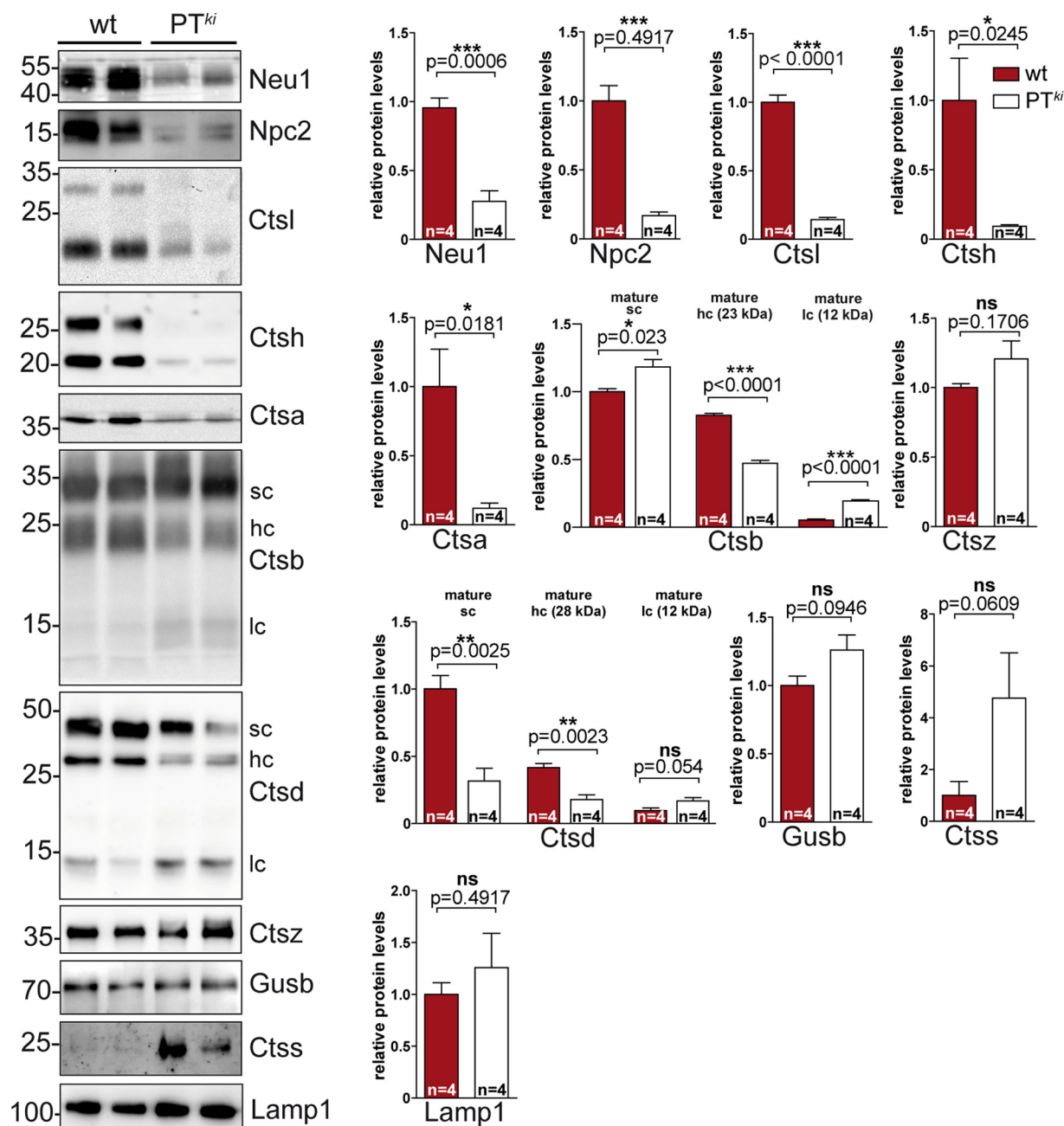
FIG. 3. **Analysis of lysosomal proteins that are specifically changed in their expression in PT^{ki} lysosomes.** Western blotting analysis for Neu1, Npc2, Ctsl, Ctsh, Ctsa, Ctsb, Ctsd, Ctsz, Gusb, Ctss, and Lamp1 in lysosome-enriched fractions from wt and PT^{ki} mice. Densitometric evaluation of the corresponding immunoreactive bands confirms the significant differences between wt and PT^{ki} samples ($n = 4$; *sc*, single chain; *hc*, heavy chain; *lc*, light chain; *ns*, not significant; $p < 0.05$, *; $p < 0.01$, **; $p < 0.001$, ***).

and Ctsd increased amounts of missorted precursor forms were detected in the medium (Fig. 5A).

To analyze targeting, sorting and processing of Ctsd and Ctsz in hepatocytes in more detail, [^{35}S] methionine pulse-chase experiments were performed. The rate of synthesis of Ctsd and Ctsz was comparable in wt and PT^{ki} hepatocytes (Fig. 5B, lane 1 and 3). During the chase period proteolytic maturation of newly synthesized Ctsd was impaired in PT^{ki} hepatocytes, and only a small portion was retained intracel-

lularly accompanied by hypersecretion of the precursor form (Fig. 5B, lane 4 and 6). During the chase Ctsz was completely missorted by PT^{ki} hepatocytes into the medium (Fig. 5B, lane 4 and 6). The presence of other lysosomal enzymes, α-L-fucosidase, β-glucuronidase, and α-L-iduronidase, were detected by measurement of their enzymatic activity in hepatocyte extracts and conditioned medium. Similar activities of these lysosomal hydrolases were detected in wt and PT^{ki} hepatocytes with the exception of α-L-fucosidase that was
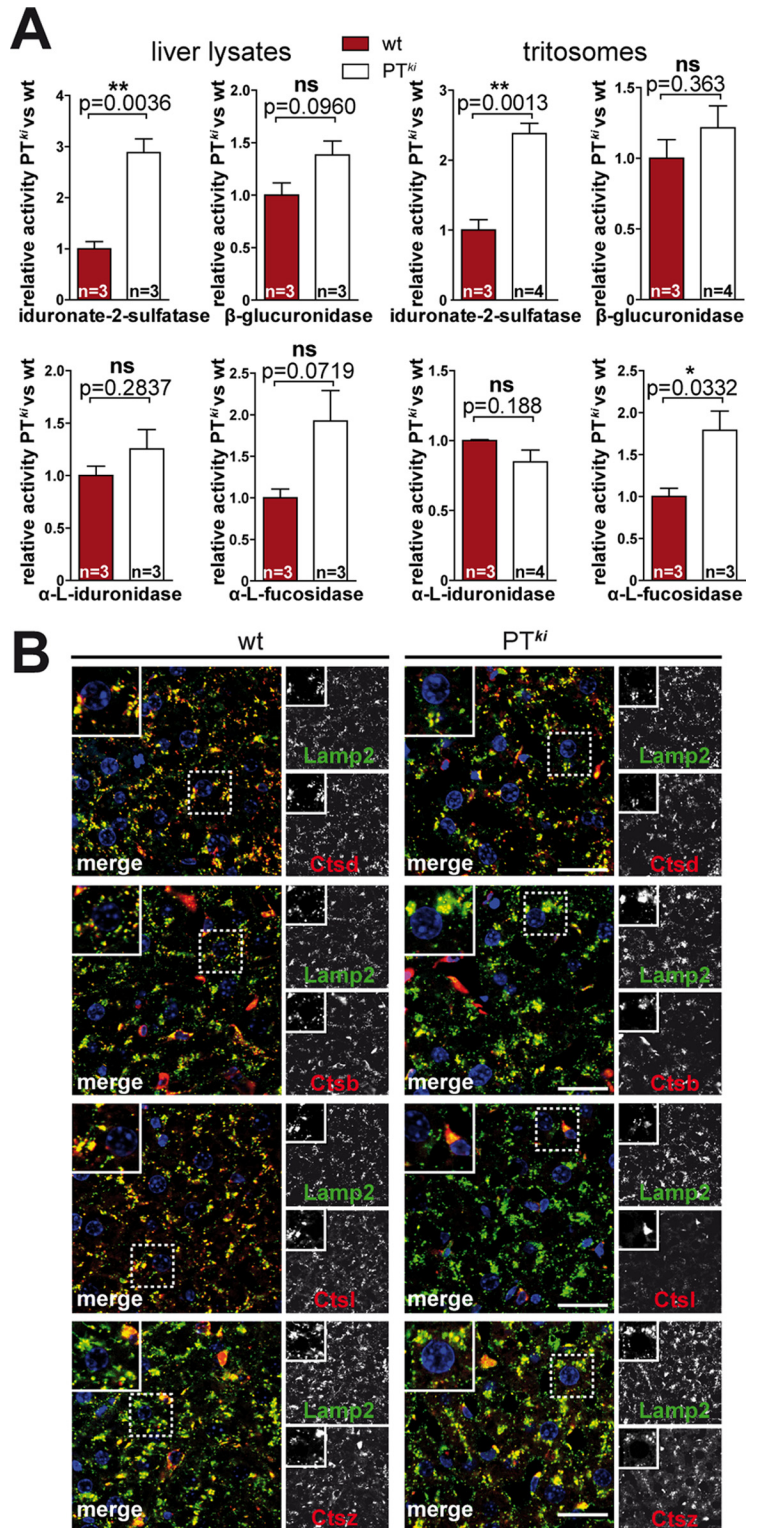
FIG. 4. **Enzymatic activity and localization of lysosomal enzymes in PT^{ki} liver.** *A*, The relative enzyme activities of iduronate-2-sulfatase, β-glucuronidase, α-L-iduronidase and α-L-fucosidase were measured in liver lysates and lysosome-enriched fractions (tritosomes). The specific activities of wt were set to 1. ns, not significant; $p < 0.05$, *; $p < 0.01$, **; $p < 0.001$, ***. *B*, Immunofluorescence staining of lysosomal proteins on liver sections. Coimmunofluorescence staining on liver sections show that Ctsd, Ctsb and Ctsz (*red*) are mainly found in Lamp2-positive structures (*green*) in both hepatocytes and nonparenchymal, whereas Ctsl is significantly reduced in PT^{ki} hepatocytes. For each panel, a hepatocyte (with large round nucleus) is shown in an *enlarged inset*. Nuclei were stained with DAPI (*blue*). *Scale bars*: 25 μm.

increased both in cells and the medium (supplemental Fig. S4B). Double immunofluorescence microscopic imaging revealed the prominent expression of Ctsd, Ctsb and Neu1 in Lamp 1-positive structures of wt and PT^{ki} hepatocytes (Fig. 5C). These data were supported by Western blotting analyses

of lysosomal proteins in cultured LSECs. The expression pattern of Neu1, Npc2, Ctsb, and Ctsz appear to be similar of those in cultured hepatocytes (supplemental Fig. S5). In contrast, the amounts and the proteolytic processing of Ctsl and Ctsd in PT^{ki} LSECs differed from cultured PT^{ki} hepatocytes,
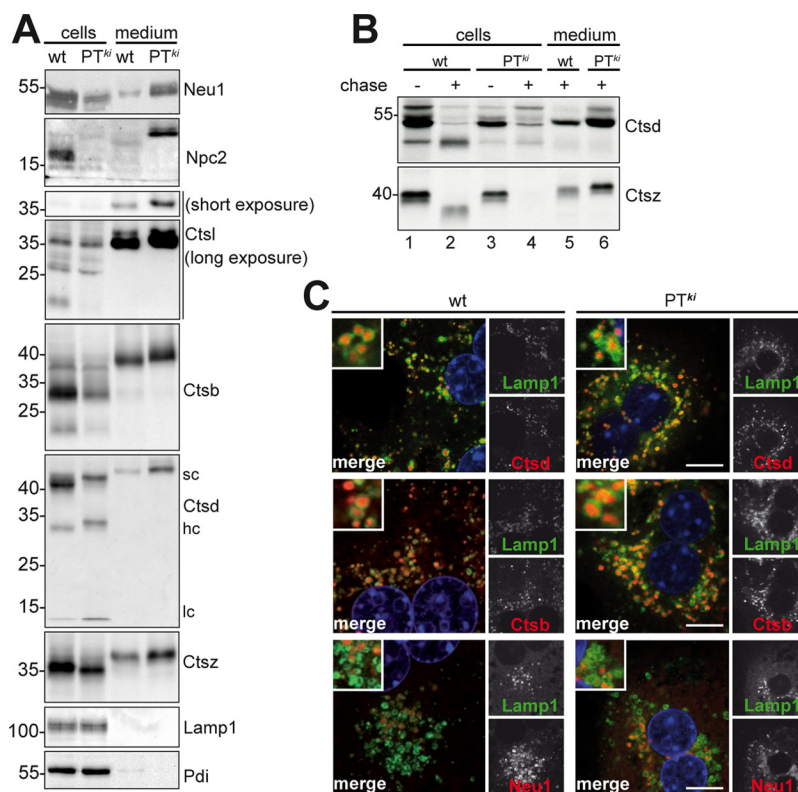
FIG. 5. **Sorting, transport and localization of lysosomal proteins in cultured PT^{ki} hepatocytes.** *A*, Isolated hepatocytes from wt and PT^{ki} mice were cultivated for 2 days and the expression of Neu1, Npc2, Ctsl, Ctsb, Ctsd, Ctsz and Lamp1 were determined by Western blotting in the cell lysates and conditioned media. The ER marker protein disulfide isomerase (Pdi) was used as loading control. All soluble lysosomal proteins are missorted to variable degree indicated by reduced intracellular levels and increased secretion into the medium. The intracellular retention of Ctsl, Ctsb and Ctsd are less affected. Comparable Lamp1 levels between wt and PT^{ki} cells are observed. *B*, Hepatocytes from wt and PT^{ki} mice were labeled with [^{35}S]-methioine for 45 min and either harvested (−, *lanes 1, 3*) or chased for 5 h (+, *lanes 2, 4*) followed by immunoprecipitation of cathepsin D (Ctsd) and cathepsin Z (Ctsz) from cell extracts (*lanes 1–4*) and media (*lanes 5–6*). The immunocomplexes were solubilized, separated by SDS-PAGE and visualized by fluorography. Secretion of newly synthesized Ctsd and Ctsz is increased in PT^{ki} hepatocytes, accompanied by a significant reduction or complete loss of processed intracellular mature forms, respectively, during the chase. *C*, Isolated hepatocytes from wt and PT^{ki} mice were fixed, and immunostained for localization of endogenous cathepsin D (*Ctsd*), cathepsin B (*Ctsb*) and neuraminidase 1 (*Neu1*) in *red* and the lysosomal marker protein Lamp1 (*green*). Nuclei were stained with DAPI (*blue*). Only merged images are shown in which *yellow* indicates colocalization of the antigens. *Magnified images* of the indicated *white rectangles* are shown in the insets. *Scale bars*: 7.5 μm.

and were rather similar to those in wt cells. Together, the expression, targeting efficiency and lysosomal localization of the most soluble lysosomal proteins tested in isolated primary hepatic cells or LSECs resemble their MS-based quantity and immuno-positive expression in tritosome fractions of wt and PT^{ki} mice.

Cargo Receptors—The majority of soluble lysosomal proteins in PT^{ki} tritosomes were found in comparable amounts as in wt controls suggesting their M6P-independent transport. Because it has been shown that in PT^{ki} fibroblasts Lrp1 and LDL receptors (Ldlr) are involved in M6P-independent targeting of nonphosphorylated lysosomal proteins (31), we have analyzed the expression of known and potential cargo receptors. No differences in the expression of Lrp1 protein have been observed in tritosome fractions, liver lysate or cultured hepatocytes between PT^{ki} and wt controls (supplemental Fig. S6A and S6B). Of note, there is an accumulation of Lrp1

fragments in PT^{ki} tritosomes. In cultured hepatocytes the amount of the Ldlr was increased most likely because of increased transcriptional activation (supplemental Fig. S6B and S6C). The total amounts of Mpr300 in PT^{ki} hepatocytes are not altered and corresponded with the relative mRNA expression level (supplemental Fig. S6B and S6C). However, the 1.8-fold higher amount of the internalized recombinant M6P-containing Mpr300 ligand, [^{125}I] arylsulfatase B (ARSB), indicated that the number of Mpr300 localized at the surface of PT^{ki} hepatocytes is increased (supplemental Fig. S6D).

DISCUSSION

This study reports on the first quantitative analysis of the lysosomal proteome of mouse liver recovering almost all known soluble lysosomal enzymes and accessory proteins. These data were compared with the lysosomal proteome from mice lacking the lysosomal targeting signal mannose 6-phos-

phate (M6P), and provided valuable insights into i) the efficiency of alternate transport systems in liver cells to prevent lysosomal dysfunctions, and ii) peripheral proteins attached transiently to the cytosolic surface of lysosomes playing an important role in lysosomal positioning, fusion, and signaling. Our approach also extended previous studies combining affinity purification of M6P-containing proteins with mass spectrometry of several tissues and lysosomal disease models (46–48) which neither allow quantitative analyses of lysosomal proteomes nor its application to cells or tissues of mucolipidosis II patients or corresponding mouse models, respectively.

The concentrations of the identified 67 known soluble lysosomal proteins comprising different classes of acidic hydrolases and accessory proteins vary over a wide range from highly abundant cathepsin D and granulin (334 and 342 nmoles/g lysosomal protein, respectively), to low abundant α-L fucosidase, iduronate 2-sulfatase, and cathepsin K (4.0, 2.1, and 2 nmoles/g, respectively). Similarly, the lysosomal integral membrane proteins Npc1, Lamp1, and Limp2 (Scarb2) represent highly abundant proteins (202, 105, and 158 nmoles/g lysosomal protein, respectively) whereas others, such as the osteopetrosis-associated transmembrane protein 1 (Ostm1), phosphatidylinositol 4,5 bisphosphate 4-phosphatase (TM55A), and presenilin1 belong to the low expressed proteins (3.7, 2.1, and 1.3 nmoles/g lysosomal protein, respectively).

Furthermore, our approach allowed the quantification of steady-state concentrations of peripheral membrane proteins on the cytoplasmic side of lysosomes involved in vesicular targeting, positioning, and signaling. Among the numerous proteins playing a role in the vesicular transport machinery (supplemental Table S5), the adaptor protein AP3 complex subunits comprised the most abundant proteins (17.4–31.7 nmoles/g lysosomal protein). In addition, five of the eight subunits of the BLOC-one-related complex (BORC) essential for lysosome positioning (49) have been identified in our preparations. Their expression ranges from 1.1 nmoles (Mef2bnb) to 6.2 nmoles/g lysosomal protein (myrlysin). In addition, rab7a and Arl8b, which have been recently reported to be involved in redistribution of lysosomes (50), belong to the more abundant peripheral proteins (11.7 and 24.2 nmoles/g lysosomal protein). Finally, we found all five Ragulator subunits LAMTOR 1 to 5 (Lysosomal Adaptor and Mitogen-activated protein kinase and mTOR activator/regulator) which interact with and recruit Rag GTPases to the lysosomal surface and mediate the translocation and activation of mTOR complex 1 (51). mTORC1 is a central component of fine tuned signaling pathways coupling internal and external stimuli (52).

The primary biochemical defect in ML II is the lack in GlcNAc-1-phosphotransferase (PT) activity that causes the inability to generate the M6P recognition marker for efficient targeting of soluble lysosomal enzymes. Therefore, fibroblasts and mesenchymal cells are deficient for a large number of lysosomal enzymes because of their hypersecretion (53). However, in certain liver cells of ML II patients such as hepatocytes or Kupffer cells, and in liver tissue of patients and PT[ki] mice nearly normal levels of few selected lysosomal enzymes were reported (17, 19, 20). In agreement with these observations, our quantitative analysis of the lysosomal proteome revealed that the concentration of only 5 out of 67 soluble proteins (Neu1, Ctsf, Npc2, Ctsl, and Smpd1) were more than 50% reduced in comparison with wild-type proteins (Table I) independent of transcriptional regulation (supplemental Fig. S3A). The proteome data were validated by Western blotting analyses of 11 soluble lysosomal enzymes in tritosome fractions (Fig. 3) and by activity measurements of four additional lysosomal enzymes (Fig. 4A). The low amounts of neuraminidase 1 (Neu1, sialidase) might lead to increased excretion of sialic acid-containing oligosaccharides in the urine as described in ML II patients (54). The loss of neuraminidase 1 from lysosomes is, however, far more severe in fibroblasts, where no activity of neuraminidase 1 in fibroblasts of three unrelated ML II patients was found (55). This has been confirmed by SILAC-based lysosomal proteome analysis of PT[ki] mouse fibroblasts that found <5% neuraminidase 1 protein compared with wild-type controls (31). It is obvious, however, that the partial loss of a few select lysosomal enzymes is not limiting for lysosome functions as demonstrated by the absence of storage material in PT[ki] liver sections by electron microscopy (supplemental Fig. S7) that is also supported by our results in cultured hepatocytes (Fig. 5 and supplemental Fig. S4) and liver sinusoid endothelial cells (supplemental Fig. S5) prepared from wild-type and PT[ki] mice. The majority (49 of 67) of luminal (Table I), integral and peripheral lysosomal proteins were not or only moderately changed in their concentration in PT[ki] lysosomal fractions (supplemental Tables S3 and S5).

The nearly normal composition of luminal proteins in liver lysosomes in the absence of M6P residues suggests that there are alternate M6P-independent targeting systems to lysosomes. Several M6P-independent receptors for the transport of lysosomal enzymes have been identified such as the LDL receptor-related protein 1 (Lrp1; (31, 43, 56, 57)), Lrp2 (megalin;(58)), LIMP-2 (59), Sortilin (60–62), SEZ6L2 (63), and mannose receptors (64). For the majority of these alternate M6P-independent receptors one or only a few lysosomal enzyme ligands have been tested or verified. Therefore it is unclear how many different receptor routes are used in liver cells of PT[ki] mice in vivo to allow the targeting of the ~60 lysosomal enzymes. At least in part, the acid hydrolases secreted by all cells of PT[ki] mice are cleared from the plasma by mannose receptors localized on macrophage-like Kupffer cells and hepatic endothelial cells (64) and exhibiting specificities for terminal mannose, GlcNAc and fucose residues (65). Additionally, the high number of LDL receptor and Lrp1 on the surface of hepatocytes most likely contribute to the re-internalization of missorted, non-phosphorylated lysosomal enzymes (31).

In summary, our lysosomal proteome analyses reveal striking protein-specific differences in the abundance of soluble

and membrane-bound proteins as well as in peripheral proteins localized on the cytosolic side of mouse liver lysosomes. The lysosomal composition and the lack of storage material in liver unable to form the major lysosomal targeting signal, mannose 6-phosphate, suggests that alternate cargo receptor routes guarantee the transport of nonphosphorylated lysosomal enzymes in sufficient amounts to maintain almost normal functions of liver cells. These observations emphasize that the lysosomal proteome must be quantified systematically in various organs and cell types in order to further our understanding of the physiological role of individual and subsets of lysosomal enzymes in cellular homeostasis.

‡‡ To whom correspondence should be addressed: University Medical Center Hamburg-Eppendorf Children's Hospital, Dept. Biochemistry, Martinistr. 52, 20251 Hamburg, Germany. Tel.: +49 40 7410 54493; E-mail: braulke@uke.de; Christian-Albrechts-Universität zu Kiel, Institut für Biochemie Olshausenstr. 40, 24098 Kiel Germany. Tel.: +49 431 880 2218; E-mail: mdamme@biochem.uni-kiel.de.

REFERENCES

1. Reitman, M. L., and Kornfeld, S. (1981) Lysosomal enzyme targeting. N-Acetylglucosaminylphosphotransferase selectively phosphorylates native lysosomal enzymes. *J. Biol. Chem.* **256,** 11977–11980

2. Reitman, M. L., and Kornfeld, S. (1981) UDP-N-acetylglucosamine:glycoprotein N-acetylglucosamine-1-phosphotransferase. Proposed enzyme for the phosphorylation of the high mannose oligosaccharide units of lysosomal enzymes. *J. Biol. Chem.* **256,** 4275–4281

3. Waheed, A., Hasilik, A., and von Figura, K. (1982) UDP-N-acetylglucosamine:lysosomal enzyme precursor N-acetylglucosamine-1-phosphotransferase. Partial purification and characterization of the rat liver Golgi enzyme. *J. Biol. Chem.* **257,** 12322–12331

4. Varki, A., and Kornfeld, S. (1980) Identification of a rat liver alpha-N-acetylglucosaminyl phosphodiesterase capable of removing "blocking" alpha-N-acetylglucosamine residues from phosphorylated high mannose oligosaccharides of lysosomal enzymes. *J. Biol. Chem.* **255,** 8398–8401

5. Ghosh, P., Dahms, N. M., and Kornfeld, S. (2003) Mannose 6-phosphate receptors: new twists in the tale. *Nat. Rev. Mol. Cell Biol.* **4,** 202–212

6. Bonifacino, J. S., and Rojas, R. (2006) Retrograde transport from endosomes to the trans-Golgi network. *Nat. Rev. Mol. Cell Biol.* **7,** 568–579

7. Bao, M., Booth, J. L., Elmendorf, B. J., and Canfield, W. M. (1996) Bovine UDP-N-acetylglucosamine:lysosomal-enzyme N-acetylglucosamine-1-phosphotransferase. I. Purification and subunit structure. *J. Biol. Chem.* **271,** 31437–31445

8. Kudo, M., Bao, M., D'Souza, A., Ying, F., Pan, H., Roe, B. A., and Canfield, W. M. (2005) The alpha- and beta-subunits of the human UDP-N-acetylglucosamine:lysosomal enzyme N-acetylglucosamine-1-phosphotransferase [corrected] are encoded by a single cDNA. *J. Biol. Chem.* **280,** 36141–36149

9. Tiede, S., Storch, S., Lubke, T., Henrissat, B., Bargal, R., Raas-Rothschild, A., and Braulke, T. (2005) Mucolipidosis II is caused by mutations in GNPTA encoding the alpha/beta GlcNAc-1-phosphotransferase. *Nat. Med.* **11,** 1109–1112

10. Raas-Rothschild, A., Cormier-Daire, V., Bao, M., Genin, E., Salomon, R., Brewer, K., Zeigler, M., Mandel, H., Toth, S., Roe, B., Munnich, A., and Canfield, W. M. (2000) Molecular basis of variant pseudo Hurler polydystrophy (mucolipidosis IIIC). *J. Clin. Invest.* **105,** 673–681

11. Qian, Y., Lee, I., Lee, W. S., Qian, M., Kudo, M., Canfield, W. M., Lobel, P., and Kornfeld, S. (2010) Functions of the alpha, beta, and gamma subunits of UDP-GlcNAc:lysosomal enzyme N-acetylglucosamine-1-phosphotransferase. *J. Biol. Chem.* **285,** 3360–3370

12. Lee, W. S., Payne, B. J., Gelfman, C. M., Vogel, P., and Kornfeld, S. (2007) Murine UDP-GlcNAc:lysosomal enzyme N-acetylglucosamine-1-phosphotransferase lacking the gamma-subunit retains substantial activity toward acid hydrolases. *J. Biol. Chem.* **282,** 27198–27203

13. De Pace, R., Velho, R. V., Encarnacao, M., Marschner, K., Braulke, T., and Pohl, S. (2015) Subunit interactions of the disease-related hexameric GlcNAc-1-phosphotransferase complex. *Hum. Mol. Genet.* **24,** 6826–6835

14. Braulke, T., Raas-Rothschild, A., Kornfeld S. (2013) I-cell disease and pseudo-Hurler polydystrophy: disorder of lysosomal enzyme phosphorylation and localization. In: In Valle D., V. B., Kinzler K.W., Antonarakis S.E., Ballabio A., Scriver C.R., Sly W.S., Bunz F., Gibson K.M., Mitchell G., ed. *The Online Metabolic and Molecular Basis of Inherited Diseases*, McGraw-Hill, New York

15. Hasilik, A., and Neufeld, E. F. (1980) Biosynthesis of lysosomal enzymes in fibroblasts. Synthesis as precursors of higher molecular weight. *J. Biol. Chem.* **255,** 4937–4945

16. Honey, N. K., Miller, A. L., and Shows, T. B. (1981) The mucolipidoses: identification by abnormal electrophoretic patterns of lysosomal hydrolases. *Am. J. Med. Genet.* **9,** 239–253

17. Kollmann, K., Damme, M., Markmann, S., Morelle, W., Schweizer, M., Hermans-Borgmeyer, I., Rochert, A. K., Pohl, S., Lubke, T., Michalski, J. C., Kakela, R., Walkley, S. U., and Braulke, T. (2012) Lysosomal dysfunction causes neurodegeneration in mucolipidosis II 'knock-in' mice. *Brain* **135,** 2661–2675

18. Leroy, J. G., Ho, M. W., MacBrinn, M. C., Zielke, K., Jacob, J., and O'Brien, J. S. (1972) I-cell disease: biochemical studies. *Pediatr. Res.* **6,** 752–757

19. Waheed, A., Pohlmann, R., Hasilik, A., von Figura, K., van Elsen, A., and Leroy, J. G. (1982) Deficiency of UDP-N-acetylglucosamine:lysosomal enzyme N-acetylglucosamine-1-phosphotransferase in organs of I-cell patients. *Biochem. Biophys. Res. Commun.* **105,** 1052–1058

20. Owada, M., and Neufeld, E. F. (1982) Is there a mechanism for introducing acid hydrolases into liver lysosomes that is independent of mannose 6-phosphate recognition? Evidence from I-cell disease. *Biochem. Biophys. Res. Commun.* **105,** 814–820

21. Glickman, J. N., and Kornfeld, S. (1993) Mannose 6-phosphate-independent targeting of lysosomal enzymes in I-cell disease B lymphoblasts. *J. Cell Biol.* **123,** 99–108

22. Kollmann, K., Pestka, J. M., Kuhn, S. C., Schone, E., Schweizer, M., Karkmann, K., Otomo, T., Catala-Lehnen, P., Failla, A. V., Marshall, R. P., Krause, M., Santer, R., Amling, M., Braulke, T., and Schinke, T. (2013) Decreased bone formation and increased osteoclastogenesis cause bone loss in mucolipidosis II. *EMBO Mol. Med.* **5,** 1871–1886

23. Otomo, T., Schweizer, M., Kollmann, K., Schumacher, V., Muschol, N., Tolosa, E., Mittrucker, H. W., and Braulke, T. (2015) Mannose 6 phosphorylation of lysosomal enzymes controls B cell functions. *J. Cell Biol.* **208,** 171–180

24. Ong, W. Y., Sundaram, R. K., Huang, E., Ghoshal, S., Kumar, U., Pentchev, P. G., and Patel, S. C. (2004) Neuronal localization and association of Niemann Pick C2 protein (HE1/NPC2) with the postsynaptic density. *Neuroscience* **128,** 561–570

25. Claussen, M., Kubler, B., Wendland, M., Neifer, K., Schmidt, B., Zapf, J., and Braulke, T. (1997) Proteolysis of insulin-like growth factors (IGF) and IGF binding proteins by cathepsin D. *Endocrinology* **138,** 3797–3803

26. Meredith, M. J. (1988) Rat hepatocytes prepared without collagenase: prolonged retention of differentiated characteristics in culture. *Cell Biol. Toxicol.* **4,** 405–425

27. Diehl, L., Schurich, A., Grochtmann, R., Hegenbarth, S., Chen, L., and Knolle, P. A. (2008) Tolerogenic maturation of liver sinusoidal endothelial cells promotes B7-homolog 1-dependent CD8+ T cell tolerance. *Hepatology* **47,** 296–305

28. Damme, M., Morelle, W., Schmidt, B., Andersson, C., Fogh, J., Michalski, J. C., and Lubke, T. (2010) Impaired lysosomal trimming of N-linked oligosaccharides leads to hyperglycosylation of native lysosomal proteins in mice with alpha-mannosidosis. *Mol. Cell. Biol.* **30,** 273–283

29. Pohl, S., and Hasilik, A. (2015) Biosynthesis, targeting, and processing of lysosomal proteins: pulse-chase labeling and immune precipitation. *Methods Cell Biol.* **126,** 63–83

30. Braulke, T., Gartung, C., Hasilik, A., and von Figura, K. (1987) Is movement of mannose 6-phosphate-specific receptor triggered by binding of lysosomal enzymes? *J. Cell Biol.* **104,** 1735–1742

31. Markmann, S., Thelen, M., Cornils, K., Schweizer, M., Brocke-Ahmadinejad, N., Willnow, T., Heeren, J., Gieselmann, V., Braulke, T., and Kollmann, K. (2015) Lrp1/LDL Receptor Play Critical Roles in Mannose 6-Phosphate-Independent Lysosomal Enzyme Targeting. *Traffic* **16,** 743–759

32. Voznyi, Y. V., Keulemans, J. L., and van Diggelen, O. P. (2001) A fluorimetric enzyme assay for the diagnosis of MPS II (Hunter disease). *J. Inherit. Metab. Dis.* **24,** 675–680

33. Distler, U., Kuharev, J., Navarro, P., Levin, Y., Schild, H., and Tenzer, S. (2014) Drift time-specific collision energies enable deep-coverage data-independent acquisition proteomics. *Nat. Methods* **11,** 167–170

34. Li, G. Z., Vissers, J. P., Silva, J. C., Golick, D., Gorenstein, M. V., and Geromanos, S. J. (2009) Database searching and accounting of multiplexed precursor and product ion spectra from the data independent analysis of simple and complex peptide mixtures. *Proteomics* **9,** 1696–1719

35. Jones, P., Cote, R. G., Martens, L., Quinn, A. F., Taylor, C. F., Derache, W., Hermjakob, H., and Apweiler, R. (2006) PRIDE: a public repository of protein and peptide identifications for the proteomics community. *Nucleic Acids Res.* **34,** D659–D663

36. Metsalu, T., and Vilo, J. (2015) ClustVis: a web tool for visualizing clustering of multivariate data using Principal Component Analysis and heatmap. *Nucleic Acids Res.* **43,** W566–570

37. Huang da, W, Sherman, B. T., and Lempicki, R. A. (2009) Systematic and integrative analysis of large gene lists using DAVID bioinformatics resources. *Nat. Protoc.* **4,** 44–57

38. Kowalewski, B., Lubke, T., Kollmann, K., Braulke, T., Reinheckel, T., Dierks, T., and Damme, M. (2014) Molecular characterization of arylsulfatase G: expression, processing, glycosylation, transport, and activity. *J. Biol. Chem.* **289,** 27992–28005

39. Hanewinkel, H., Glossl, J., and Kresse, H. (1987) Biosynthesis of cathepsin B in cultured normal and I-cell fibroblasts. *J. Biol. Chem.* **262,** 12351–12355

40. Silva, J. C., Gorenstein, M. V., Li, G. Z., Vissers, J. P., and Geromanos, S. J. (2006) Absolute quantification of proteins by LCMSE: a virtue of parallel MS acquisition. *Mol. Cell. Proteomics* **5,** 144–156

41. Schroder, B. A., Wrocklage, C., Hasilik, A., and Saftig, P. (2010) The proteome of lysosomes. *Proteomics* **10,** 4053–4076

42. Lubke, T., Lobel, P., and Sleat, D. E. (2009) Proteomics of the lysosome. *Biochim. Biophys. Acta* **1793,** 625–635

43. Zhou, X., Sun, L., Bastos de Oliveira, F., Qi, X., Brown, W. J., Smolka, M. B., Sun, Y., and Hu, F. (2015) Prosaposin facilitates sortilin-independent lysosomal trafficking of progranulin. *J. Cell Biol.* **210,** 991–1002

44. Sleat, D. E., Sun, P., Wiseman, J. A., Huang, L., El-Banna, M., Zheng, H., Moore, D. F., and Lobel, P. (2013) Extending the mannose 6-phosphate glycoproteome by high resolution/accuracy mass spectrometry analysis of control and acid phosphatase 5-deficient mice. *Mol. Cell. Proteomics* **12,** 1806–1817

45. Chapel, A., Kieffer-Jaquinod, S., Sagne, C., Verdon, Q., Ivaldi, C., Mellal, M., Thirion, J., Jadot, M., Bruley, C., Garin, J., Gasnier, B., and Journet, A. (2013) An extended proteome map of the lysosomal membrane reveals novel potential transporters. *Mol. Cell. Proteomics* **12,** 1572–1588

46. Czupalla, C., Mansukoski, H., Riedl, T., Thiel, D., Krause, E., and Hoflack, B. (2006) Proteomic analysis of lysosomal acid hydrolases secreted by osteoclasts: implications for lytic enzyme transport and bone metabolism. *Mol. Cell. Proteomics* **5,** 134–143

47. Sleat, D. E., Lackland, H., Wang, Y., Sohar, I., Xiao, G., Li, H., and Lobel, P. (2005) The human brain mannose 6-phosphate glycoproteome: a complex mixture composed of multiple isoforms of many soluble lysosomal proteins. *Proteomics* **5,** 1520–1532

48. Qian, M., Sleat, D. E., Zheng, H., Moore, D., and Lobel, P. (2008) Proteomics analysis of serum from mutant mice reveals lysosomal proteins selectively transported by each of the two mannose 6-phosphate receptors. *Mol. Cell. Proteomics* **7,** 58–70

49. Pu, J., Schindler, C., Jia, R., Jarnik, M., Backlund, P., and Bonifacino, J. S. (2015) BORC, a multisubunit complex that regulates lysosome positioning. *Dev. Cell* **33,** 176–188

50. Johnson, D. E., Ostrowski, P., Jaumouille, V., and Grinstein, S. (2016) The position of lysosomes within the cell determines their luminal pH. *J. Cell Biol.* **212,** 677–692

51. Sancak, Y., Bar-Peled, L., Zoncu, R., Markhard, A. L., Nada, S., and Sabatini, D. M. (2010) Ragulator-Rag complex targets mTORC1 to the lysosomal surface and is necessary for its activation by amino acids. *Cell* **141,** 290–303

52. Bar-Peled, L., and Sabatini, D. M. (2014) Regulation of mTORC1 by amino acids. *Trends Cell Biol.* **24,** 400–406

53. Hickman, S., and Neufeld, E. F. (1972) A hypothesis for I-cell disease: defective hydrolases that do not enter lysosomes. *Biochem. Biophys. Res. Commun.* **49,** 992–999

54. Strecker, G., Peers, M. C., Michalski, J. C., Hondi-Assah, T., Fournet, B., Spik, G., Montreuil, J., Farriaux, J. P., Maroteaux, P., and Durand, P. (1977) Structure of nine sialyl-oligosaccharides accumulated in urine of eleven patients with three different types of sialidosis. Mucolipidosis II and two new types of mucolipidosis. *Eur. J. Biochem.* **75,** 391–403

55. Thomas, G. H., Tiller, G. E., Jr, Reynolds, L. W., Miller, C. S., and Bace, J. W. (1976) Increased levels of sialic acid associated with a sialidase deficiency in I-cell disease (mucolipidosis II) fibroblasts. *Biochem. Biophys. Res. Commun.* **71,** 188–195

56. Hiesberger, T., Huttler, S., Rohlmann, A., Schneider, W., Sandhoff, K., and Herz, J. (1998) Cellular uptake of saposin (SAP) precursor and lysosomal delivery by the low density lipoprotein receptor-related protein (LRP). *EMBO J.* **17,** 4617–4625

57. Beaujouin, M., Prebois, C., Derocq, D., Laurent-Matha, V., Masson, O., Pattingre, S., Coopman, P., Bettache, N., Grossfield, J., Hollingsworth, R. E., Zhang, H., Yao, Z., Hyman, B. T., van der Geer, P., Smith, G. K., and Liaudet-Coopman, E. (2010) Pro-cathepsin D interacts with the extracellular domain of the beta chain of LRP1 and promotes LRP1-dependent fibroblast outgrowth. *J. Cell Sci.* **123,** 3336–3346

58. Nielsen, R., Courtoy, P. J., Jacobsen, C., Dom, G., Lima, W. R., Jadot, M., Willnow, T. E., Devuyst, O., and Christensen, E. I. (2007) Endocytosis provides a major alternative pathway for lysosomal biogenesis in kidney proximal tubular cells. *Proc. Natl. Acad. Sci. U.S.A.* **104,** 5407–5412

59. Reczek, D., Schwake, M., Schroder, J., Hughes, H., Blanz, J., Jin, X., Brondyk, W., Van Patten, S., Edmunds, T., and Saftig, P. (2007) LIMP-2 is a receptor for lysosomal mannose-6-phosphate-independent targeting of beta-glucocerebrosidase. *Cell* **131,** 770–783

60. Prabakaran, T., Nielsen, R., Satchell, S. C., Mathieson, P. W., Feldt-Rasmussen, U., Sorensen, S. S., and Christensen, E. I. (2012) Mannose 6-phosphate receptor and sortilin mediated endocytosis of alpha-galactosidase A in kidney endothelial cells. *PLoS ONE* **7,** e39975

61. Lefrancois, S., Zeng, J., Hassan, A. J., Canuel, M., and Morales, C. R. (2003) The lysosomal trafficking of sphingolipid activator proteins (SAPs) is mediated by sortilin. *EMBO J.* **22,** 6430–6437

62. Hu, F., Padukkavidana, T., Vaegter, C. B., Brady, O. A., Zheng, Y., Mackenzie, I. R., Feldman, H. H., Nykjaer, A., and Strittmatter, S. M. (2010) Sortilin-mediated endocytosis determines levels of the frontotemporal dementia protein, progranulin. *Neuron* **68,** 654–667

63. Boonen, M., Staudt, C., Gilis, F., Oorschot, V., Klumperman, J., and Jadot, M. (2016) Cathepsin D and its newly identified transport receptor SEZ6L2 can modulate neurite outgrowth. *J. Cell Sci.* **129,** 557–568

64. Lee, S. J., Evers, S., Roeder, D., Parlow, A. F., Risteli, J., Risteli, L., Lee, Y. C., Feizi, T., Langen, H., and Nussenzweig, M. C. (2002) Mannose receptor-mediated regulation of serum glycoprotein homeostasis. *Science* **295,** 1898–1901

65. Schlesinger, P., Rodman, J. S., Frey, M., Lang, S., and Stahl, P. (1976) Clearance of lysosomal hydrolases following intravenous infusion. The role of liver in the clearance of beta-glucuronidase and N-acetyl-beta-D-glucosaminidase. *Arch Biochem. Biophys.* **177,** 606–614